Ceramics International 30 (2004) 1819–1822

CERAMICS INTERNATIONAL

www.elsevier.com/locate/ceramint

A low temperature nano-structured $SrTiO_3$ thick film oxygen gas sensor

Y. Hu [a], O.K. Tan [a,*], W. Cao [b], W. Zhu [a]

[a] *Sensors and Actuators Laboratory, Microelectronics Centre, School of EEE, Nanyang Technological University, 50 Nanyang Avenue, Singapore 639798, Singapore*

[b] *Singapore Institute of Manufacturing Technology, 71 Nanyang Drive, Singapore 638075, Singapore*

Received 28 November 2003; received in revised form 14 December 2003; accepted 22 December 2003

Available online 6 May 2004

Abstract

A low temperature nano-structured Strontium Titanate ($SrTiO_3$) thick film oxygen gas sensors were obtained by high-energy ball milling technique and thick-film screen-printing technique. $SrTiO_3$ nano-sized powders of around 20 nm were produced from commercial $SrTiO_3$ and synthesized $SrTiO_3$. The material micro-structural properties and sensor oxygen sensing properties were characterized using X-ray diffraction (XRD) and gas sensing measurements respectively. Experimental results show that the sensing property of the synthesized $SrTiO_3$ sensors with an annealing temperature of 400 °C is much better than the commercial $SrTiO_3$ sensors (both milled and not milled materials). Especially, their optimal operating temperature of around 40 °C is the lowest reported value for such metal oxide semiconductor gas sensors ever achieved.

Keywords: $SrTiO_3$ nano-sized powders; Low temperature; Oxygen gas sensors

1. Introduction

Strontium Titanate ($SrTiO_3$) is a very important material for oxygen sensors. It has attracted much attention because of their low cost and strong stability in thermal and chemical atmospheres [1–3]. Most research works focus on bulk-conduction-type in $SrTiO_3$ with high operating temperatures (700–1000 °C) [4], and their $SrTiO_3$ sensing material are produced by the conventional high temperature solid-state reaction method because of its high melting point (2080 °C) [5–10]. The high temperature solid-state reaction method has several problems relating to large grain growth, change in stoichiometry, and ease of second phase formation. Hence nano-size type of material in $SrTiO_3$ is difficult to be produced by this method. For $SrTiO_3$ oxygen sensors that operate at low temperatures, the surface conduction type in $SrTiO_3$ must be obtained. As shown in Fig. 1, when the grain size is small enough (the actual grain size D is less than two times the space-charge depth L), the material resistivity is determined solely by grain control, and the material conduction type becomes surface conduction type [11]. The key factor is to obtain nano-size materials for good low temperature oxygen gas sensors. The high-energy ball milling or mechanical alloying has been proved to be a very effective route to prepare nano-sized solid solution for gas sensor application recently [12–15]. In our work, $SrTiO_3$ nano-size powders are produced from commercial $SrTiO_3$ and synthesized $SrTiO_3$ at room temperature using the high-energy ball milling technique. The thick film technology is adopted to fabricate the sensor devices. Their powder particle sizes, micro-structural properties, and oxygen sensing properties are systematically studied.

2. Experimental procedure

$SrTiO_3$ nano-size powders were produced from commercial $SrTiO_3$ and synthesized $SrTiO_3$ at room temperature using high-energy ball milling in a Fritsch Pulverisette 5 planetary ball milling system. The structure of these samples was characterized using a SHIMADZU XRD-6000 X-ray diffractometer with Cu Kαl radiation (1.54056 Å) The diffractometer range, 2θ, was from 10 to 100° with a sweep rate of 4°/min. The samples (sample A: commercial $SrTiO_3$ (no milling), B: commercial $SrTiO_3$ (120 h milling

* Corresponding author. Tel.: +65-6790-5411; fax: +65-6791-2687.
E-mail address: eoktan@ntu.edu.sg (O.K. Tan).

0272-8842/$30.00
doi:10.1016/j.ceramint.2003.12.068

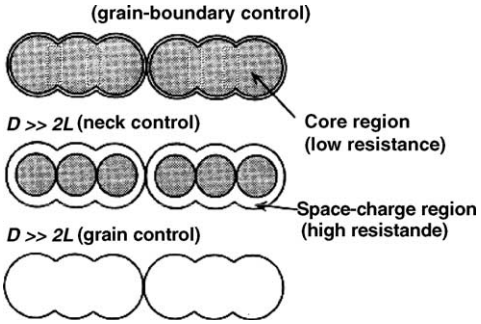

Fig. 1. Schematic models for grain-size effects [11]. *D*, the actual grain size; *L*, the space-charge depth.

time), and C: synthesized $SrTiO_3$ (120 h milling time)) were formed into pastes using the commercial organic vehicle 400 from ESL and screen-printed onto the Al_2O_3 substrates with interdigital Au electrodes. The prepared sensor devices were then annealed at the temperature of 400 °C. Their gas sensing properties were characterized using a Keithley 236 source measurement unit in the custom-designed gas sensing characterization system programmed using the National Instruments' LABVIEW version 5.0. The carrier gas was nitrogen and test gas was oxygen.

3. Results and discussion

3.1. Synthesis of $SrTiO_3$ nano-sized powders

Fig. 2(a and b) shows the XRD patterns for commercial $SrTiO_3$ and synthesized $SrTiO_3$ samples after different milling times, respectively. Fig. 2(b) shows that $SrTiO_3$ structure material with a cubic perovskite phase has been achieved while Fig. 2(a) indicates that the perovskite phase has been maintained throughout the milling process.

From the XRD peaks, the average grain size is calculated using the Scherrer equation of $B = \lambda\zeta/(d_c \cos\theta)$ [16] (deducting broadening error due to the instrument itself). Where B in radians is the broadening of the diffraction peak due purely to crystalline size measured at half of its maximum intensity; λ is the wavelength of radiation; θ is the Bragg angle; d_c is the diameter of crystalline size; and ζ is a constant 0.9, which depends mainly on the crystalline shape and indices.

Based on this principle, the average grain sizes are calculated for the different sample powders milled for different hours and shown in Fig. 3. All the sample powders go through the four stages of the mechanical alloying process, namely—(a) initial stage; (b) intermediate stage; (c) final stage; (d) completion stage [16]. At the completion stage, the new chemical bond ($SrTiO_3$ Perovskite) is formed. The grain size shows a slight increase from 20 to 80 h. It is possible that the powder particles possess an extremely deformed metastable structure at 20 h, and the surface stress of the powder particles is slowly released between 20–80 h. After 80 h, the grain size remains stable (about 20 nm).

3.2. Characterization of sensors

3.2.1. Relative resistances of the devices

The changes of relative resistance ($R_{nitrogen}/R_{oxygen}$) of the devices to 20% of oxygen gas are characterized. Sample A exhibits no sensing property as it is an insulator material. The relative resistance of sample C is higher than that of Sample B as shown in Fig. 4. The optimal relative resistance value of 6.35 is obtained for sample C operating at 40 °C. Both samples B and C have the same optimal operating temperature of 40 °C. This optimal operating temperature is much lower than the normally lower operating temperature type of semiconducting gas sensors (300–500 °C) [4].

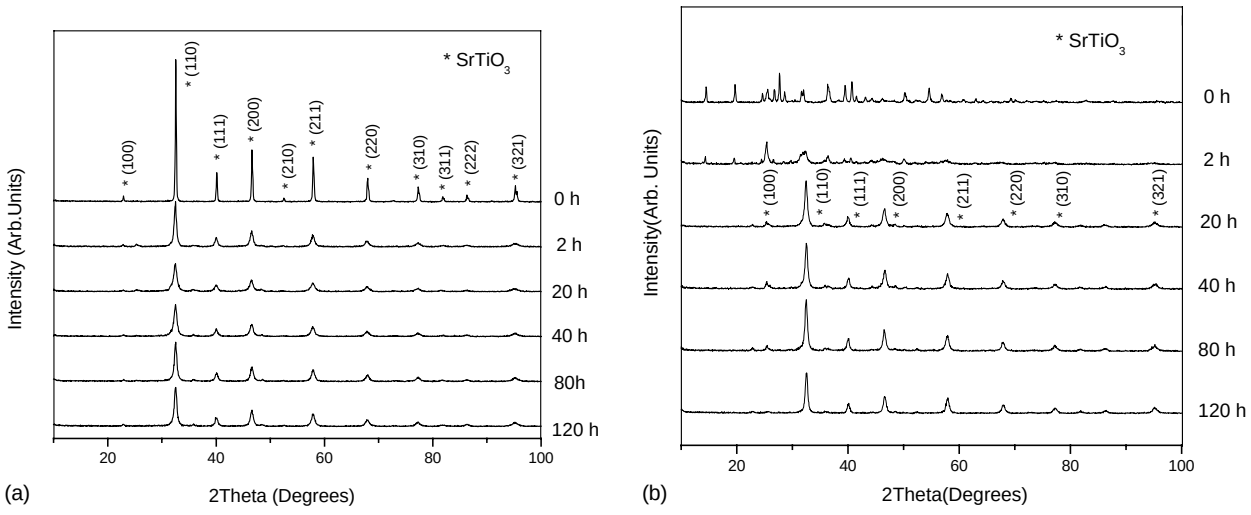

Fig. 2. XRD patterns for (a) commercial $SrTiO_3$ and (b) synthesized $SrTiO_3$ samples after different milling times.

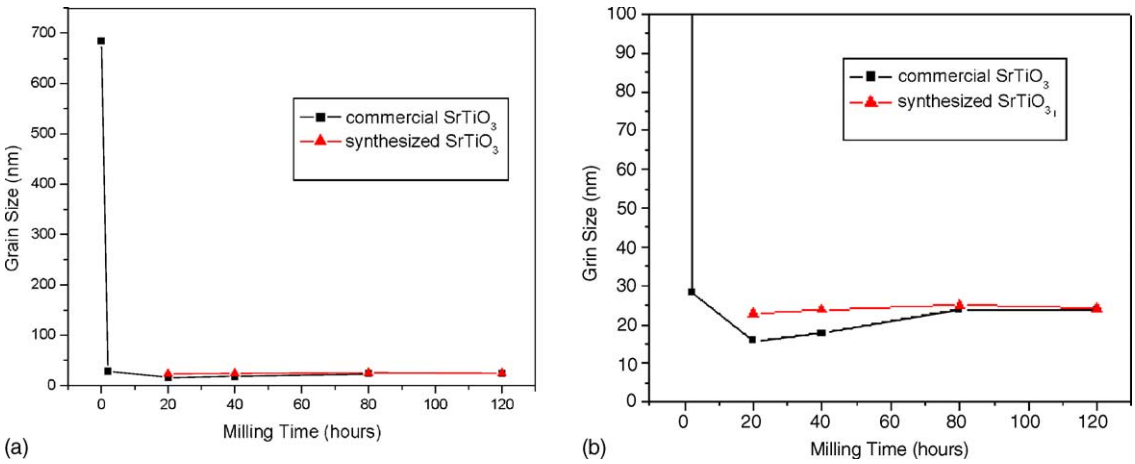

Fig. 3. Average grain size for (a) the different powders milled for different hours and (b) showing the room-in detail.

3.2.2. *Variation of relative resistance of the device with gas concentration*

The relative resistances of sample C operating at 40 °C are measured for different concentrations from 10^4 ppm to 2×10^5 ppm oxygen (air composition) and plotted in Fig. 5. At 10^4 ppm, the gas relative resistance is 2.3, and at 2×10^5 ppm oxygen, the highest relative resistance 6.35 is obtained. This is comparable to the reported relative resistance of doped $SrTiO_3$ series oxygen gas sensors with operating temperature at 700–800 °C [5,8,12]. This provides a very wide concentration range for our oxygen sensor devices.

At low oxygen concentrations the gas relative resistance value increases rapidly with the increase in the oxygen concentration, however, at higher concentrations, the increase in the gas relative resistance value becomes more gradual. This can be explained by the fact that the gas relative resistance value to a sample has a saturation value because there is a fixed surface area for each sample. When oxygen concentration on surface of the sample increases to a certain level, the oxygen molecules will cover all the surfaces of the sample, and the gas relative resistance value will reach a saturation value. The surface reactions on the sample have reached the saturation point at this stage. Further increase in oxygen concentration will not result in further increase in the gas relative resistance value.

3.2.3. *Response time*

When an input signal goes through a well defined change, the output response is defined by the time interval between the 10 and 90% of the stationary value [17]. To investigate the response time and sensing reversibility, Sample C is used. Fig. 6 depicts the response curve of the sensor undergoing the change from N_2 to 20% O_2 (N_2 as the carrier gas), and back to N_2 ambient. The response time is 1.6 min and the recovery time is 5 min. There are no semiconducting oxygen gas sensors that operate at this low temperature. Only the practical Calvanic cell-type sensor operates at room temperature but it has high ionic conduction and is often difficult to predict its sensor response.

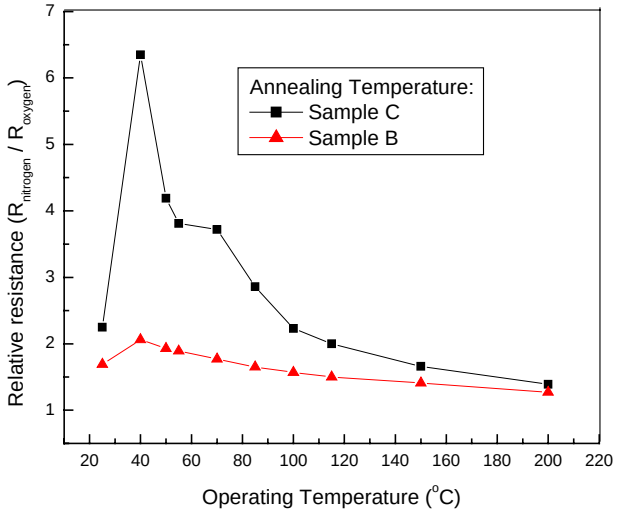

Fig. 4. Relative resistance of 120-h milled commercial $SrTiO_3$ and synthesized $SrTiO_3$ for different operating temperatures.

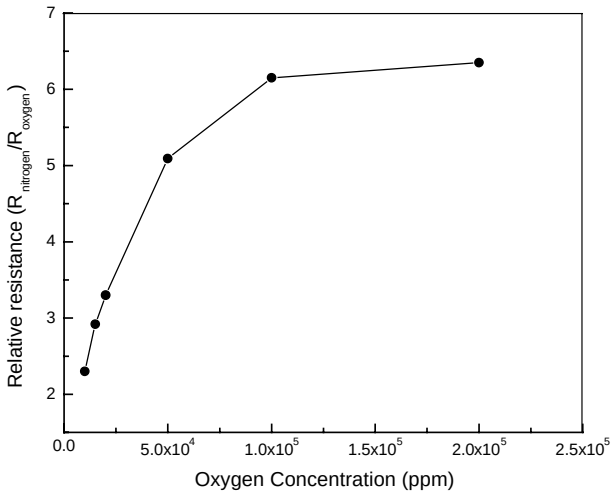

Fig. 5. The gas relative resistance vs. oxygen concentration.

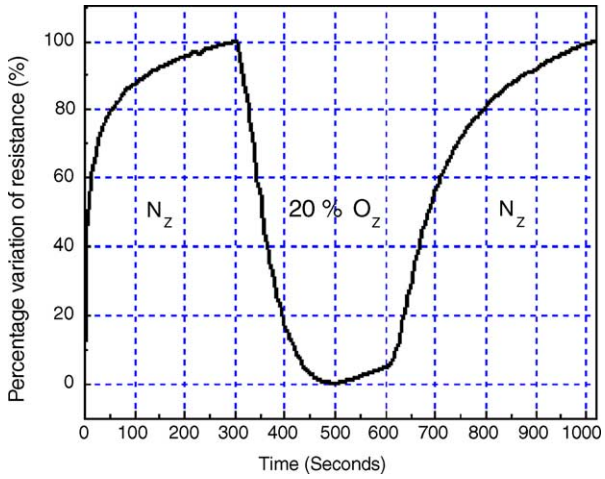

Fig. 6. Response curve of synthesized $SrTiO_3$ sample with annealing at 400 °C and operating at 40 °C.

4. Conclusion

The high-energy ball milling technique is an effective way to synthesize of $SrTiO_3$ nano-sized powders. The sensing property of the synthesized sensors with annealing temperature at 400 °C is much better than the commercial $SrTiO_3$ sensors (both milled and not milled materials). Their optimal operating temperature is found to be at about 40 °C that is close to the human body temperature. This is the lowest operating temperature reported for such metal oxide semiconductor gas sensors. The highest relative resistance for the nano-structured synthesized $SrTiO_3$ sensor devices to 20% oxygen is found to be at a value of 6.35 that is comparable to the reported relative resistance of doped $SrTiO_3$ series oxygen gas sensors with operating temperature at 700–800 °C. The response and recovery times are 1.6 and 5 min, respectively. This is fast for a room temperature operated sensor device. The detected range is 1–20% oxygen that is a very wide range possible for a single type of sensor material.

References

[1] J. Gerblinger, K.H. Hardtl, H. Meixner, R. Aigner, High-temperature microsensors, in: W. Gopel (Ed.), Sensors, A Comprehensive Survey, vol. 8, Weinheim, 1995, pp. 181–219.

[2] R. Moos, T. Bischoff, W. Menesklou, K.H. Hardtl, Solubility of lanthanum in strontium titanate in oxygen-rich atmospheres, J. Mater. Sci. 32 (1997) 4247–4252.

[3] S. Steinsvik, R. Bugge, J. Gjonnes, J. Tafto, T. Norby, The defect structure of $SrTi_{1-x}Fe_xO_{3-y}$ ($x = 0$–0.8) investigated by electrical conductivity measurements and electron energy loss spectroscopy (EELS), J. Phys. Chem. Solids 58 (6) (1997) 969–976.

[4] Y.L. Xu, X.H. Zhou, O. Toft Sørensen, Oxygen sensors based on semiconducting metal oxides: an overview, Sens. Actuators B 65 (2000) 2–4.

[5] X.H. Zhou, O. Toft Sørensen, Y.L. Xu, Defect structure and oxygen sensing properties of Mg-doped $SrTiO_3$ thick film sensors, Sens. Actuators B 41 (1997) 177–182.

[6] W. Menesklou, H.-J. Schreiner, K.H. Hardtl, E. Ivers-Tiffee, High temperature oxygen sensors based on doped $SrTiO_3$, Sens. Actuators B 59 (1999) 184–189.

[7] R. Moos, W. Menesklou, H.-J. Schreiner, K.H. Hardtl, Materials for temperature independent resistive oxygen sensors for combustion exhaust gas control, Sens. Actuators B 67 (2000) 178–183.

[8] X. Zhou, O. Toft Sørensen, Q. Cao, Y. Xu, Electrical conduction and oxygen sensing mechanism of Mg-doped $SrTiO_3$ thick film sensors, Sens. Actuators B 65 (2000) 52–54.

[9] A.J. Feighery, J.C.C. Abrantes, J.A. Labrincha, J.M.F. Ferreira, J.R. Frade, Microstructural effects on the electrical behaviour of $SrTi_{0.95}Nb_{0.05}O_{3+\delta}$ materials on changing from reducing to oxidizing conditions, Sens. Actuators B 75 (2001) 88–94.

[10] T. Ding, W. Jia, Electrophoretic deposition of $SrTi_{1-x}Mg_xO_{3-\delta}$ films in oxygen sensor, Sens. Actuators B 82 (2002) 284–286.

[11] C. Xu, J. Tamaki, N. Miura, N. Yamazor, Grain size effects on gas sensitivity of porous SnO_2-based elements, Sens. Actuators B 3 (1991) 147–155.

[12] O.K. Tan, W. Cao, W. Zhu, Alcohol sensor based on a non-equilibrium nanostructured $xZrO_2$–$(1-x)(\alpha\text{-}Fe_2O_3)_{0.2}$ solid solution system, Sens. Actuators B 63 (1–2) (2000) 129–134.

[13] W. Cao, O.K. Tan, W. Zhu, B. Jiang, Mechanical alloying and thermal decomposition of $(ZrO_2)_{0.8}$–$(\alpha\text{-}Fe_2O_3)_{0.2}$ powder for gas sensing applications, J. Solid State Chem. 155 (2000) 320–325.

[14] J.Z. Jiang, S.W. Lu, Y.X. Zhou, S. Mϕrup, K. Nielsen, E.W. Poulsen, F.J. Berry, J. McMannus, Correlation of gas sensitive properties with Fe_2O_3–SnO_2 ceramic microstructure prepared by high energy ball milling, Mater. Sci. Forum 235-238 (1997) 941–946.

[15] J.Z. Jiang, R. Lin, W. Lin, K. Nielsen, S. M?rup, K. Dam-Johansen, R. Clasen, Gas sensitive properties and structure of nanostructured $(aFe_2O_3)x$–$(SnO_2)1-x$ materials prepared by mechanical alloying, J. Phys. D: Appl. Phys. 30 (1997) 1459–1467.

[16] L. Lü, M.O. Lai, Mechanical Alloying, Kluwer Academic Publishers, 1998, pp. 11–21.

[17] A. D'amico, C. Di Natale, A. Taroni, Sensors parameters, in: Proceedings of the First European School on Sensors (ESS'94) on Sensors for domestic applications, Castro Marina, Leee, Italy, 12–17 September 1994, pp. 3–13.